Probing the Folding Intermediate of *Bacillus subtilis* RNase P Protein by Nuclear Magnetic Resonance[†]

Yu-Chu Chang, William R. Franch, and Terrence G. Oas*

Department of Biochemistry, Box 3711, Duke University Medical Center, Durham, North Carolina 27710, United States

ABSTRACT: Protein folding intermediates are often imperative for overall folding processes and consequent biological functions. However, the low population and transient nature of the intermediate states often hinder their biochemical and biophysical characterization. Previous studies have demonstrated that *Bacillus subtilis* ribonuclease P protein (P protein) is conformationally heterogeneous and folds with multiphasic kinetics, indicating the presence of an equilibrium and kinetic intermediate in its folding mechanism. In this study, nuclear magnetic resonance (NMR) spectroscopy was used to study the ensemble corresponding to this intermediate (I). The results indicate that the N-terminal and C-terminal helical regions are mostly unfolded in I. $^1H-^{15}N$ heteronuclear single-quantum coherence NMR spectra collected as a function of pH suggest that the protonation of His 22 may play a major role in the energetics of the equilibria among the unfolded, intermediate, and folded state ensembles of P protein. NMR paramagnetic relaxation enhancement experiments were also used to locate the small anion binding sites in both the intermediate and folded ensembles. The results for the folded protein are consistent with the previously modeled binding regions. These structural insights suggest a possible role for I in the RNase P holoenzyme assembly process.

An understanding of the processes by which a protein folds into its folded conformation requires knowledge of the various states that populate the folding pathways, the kinetic rate constants between these states, and their relative stabilities, as well as their structural properties. Despite the observation that many proteins fold through an intermediate state (*1−3*), the role of intermediates in productive folding is still the subject of fertile literature discussion (*4*). Intermediates between the unfolded and folded states may enhance the rate of folding by decreasing the conformational space through which the polypeptide chain has to search or may reduce the rate of folding by sequestering the polypeptide chain in a stable, partially folded state (*5, 6*).

RNase P protein (P protein) is the protein subunit in the RNase P holoenzyme. Our previous studies have established that P protein is an intrinsically disordered protein (IDP). Without the binding partners, P protein is predominantly unfolded but can be induced to fold in the presence of different small anions (e.g., sulfate). Many protein subunits in the ribonucleoprotein complexes exhibit conformational dynamics, which promote specific recognition of cognate RNA partners (*7*). The N-terminal RNA recognition domain (RRM) of human U1A binds to the 3′ untranslated region (3′-UTR) of U1A mRNA. In the absence of RNA, backbone and side chain relaxation experiments reveal conformational heterogeneity on the microsecond to millisecond time scale in the regions that bind RNA (*8, 9*). Previous nuclear magnetic resonance (NMR) studies showed that there are extra peaks in the $^1H-^{15}N$ heteronuclear single-quantum coherence (HSQC) spectrum of the sulfate-folded state of P protein, which

is evidence of alternative conformations under these conditions (*10*). Backbone dynamics studies of the sulfate-folded state of P protein under similar conditions also detected conformational heterogeneity (arising from motions on the microsecond to second time scale) (*11*). In addition, our recent kinetic and equilibrium studies of trimethylamine *N*-oxide (TMAO)-induced folding of P protein established that there is an intermediate state in the folding process (kinetic studies of sulfate-induced folding also detect an intermediate) (ref *12* and unpublished data). Assembly of ribonucleoprotein complexes is usually accompanied by conformational changes in both protein and RNA components (*13, 14*). The folding intermediates of protein or RNA components can be crucial to the overall assembly process. The absence of key intermediate states could result in non-native and misfolded ribonucleoprotein complexes (*15*). Therefore, a primary motivation for structurally and energetically characterizing this intermediate in the P protein system is to understand its role in the folding process and ultimately holoenzyme assembly.

For most small proteins, intermediates form within the dead time of a stopped-flow instrument, so it has not been feasible to determine their role in the folding process (*16, 17*). Recent development of ultrarapid mixing (*18, 19*) and temperature-jump (*20*) instruments enabled the direct detection of the initial folding phase and early folding events. The intermediate ensemble formed early in the folding of Im7 (*2*) and that of GB1 (*21*) have been shown to be on the folding pathway. In addition to the short lifetime of intermediate states, many of them are populated at very low levels, making their experimental characterization difficult in some systems. Most of the transient techniques that have been used to study protein folding are based on the use of a single probe or a single average property derived from many residues in the protein. It is thus difficult to obtain residue-specific information about the intermediate state. Therefore,

*To whom correspondence should be addressed: Department of Biochemistry, Box 3711, Duke University Medical Center, Durham, NC 27710. Telephone: (919) 684-4363. Fax: (919) 684-8885. E-mail: oas@duke.edu.

Published on Web 09/15/2010

determination of the conformational properties of an intermediate state at high resolution is important for a full elucidation of the structural mechanism of folding. However, the transient nature and low population of the intermediate states relative to the unfolded and folded state are challenges for structural experiments.

A variety of NMR methods are available and designed for the study of the conformational properties of intermediate states. Relaxation dispersion NMR spectroscopy is extremely sensitive to processes that involve interconversion between a ground state (folded or unfolded state) and excited states (intermediate state) of molecules (*22−24*). The method also provides residue-specific information over the whole protein simultaneously. NMR analysis of partially folded proteins stabilized by changing solution conditions or mutagenesis has also provided insights into the nature of their conformational ensemble (*25−27*). Another approach to investigate protein folding at the residue level is to record a series of ^{1}H−^{15}N HSQC spectra at increasing denaturant concentrations under equilibrium conditions (*28, 29*). Lastly, NMR spectroscopy provides a powerful method for monitoring the exchange of a nucleus between different environments because of conformational transitions (*30*). If the transition rate (k) is in the fast-exchange regime ($\Delta\omega \ll k$, where $\Delta\omega$ is the resonant frequency difference for the same nucleus in two magnetically inequivalent sites), a single sharp peak is observed. If the rate is in the intermediate-exchange regime ($\Delta\omega \approx k$), the peaks become very broad and can have an intensity similar to that of baseline noise. When the rate is in the slow-exchange regime ($\Delta\omega \gg k$), two resonances arising from the two distinct environments of the nucleus are observed. In this study, all three scenarios were observed in folded and unfolded P protein NMR HSQC spectra, which enabled us to structurally characterize the intermediate state of P protein. Moreover, $\Delta\omega$ values were useful for deducing structural characteristics of the intermediate. Overall, NMR offers several different ways to characterize the intermediate state kinetically, thermodynamically, and structurally.

In this study, standard multidimensional NMR experiments were performed to determine the residue identities of the extra peaks in the ^{1}H−^{15}N HSQC spectrum of the sulfate-folded state of P protein. The assignment results showed that most of these residues are located in the vicinity of the N- and C-termini and their second resonances arise from the random-coil conformation. The NMR data suggest that the central β-sheet and α-helix B are folded in the intermediate state and that the N-terminal α-helix A and C-terminal α-helix C are unfolded. Acid titration monitored by HSQC spectra indicated that histidine protonation of predominantly His 22 shifts the conformational equilibria of P protein at low pH.

EXPERIMENTAL PROCEDURES

Chemicals and Reagents. Ultrapure urea was purchased from Nacalai Tesque Inc. [^{15}N]Ammonium chloride (99%), [^{13}C]glucose (U-^{13}C$_6$, 99%), and deuterated TMAO (d$_9$, 98%) were purchased from Cambridge Isotope Laboratories Inc. Urea and TMAO concentrations were measured by refractive index using the equations from refs *31* and *32*, respectively.

Protein Mutagenesis, Expression, and Purification. Histidine variants of P protein were generated in an F107W background. These site-directed mutational plasmids were constructed using the QuikChange procedure (Stratagene) with primers GGAGATATACCATGGCTAAGCTGAAAAAACGC and

GCGTTTTTTCAGCTTAGCCATGGTATATCTCC for H3K, CCAGAAAGTGTTTAAAAAGGGGACATCAGTTGC and GCAACTGATGTCCCCTTTTTAAACACTTTCTGG for H22K, and CGAAAAAAAGTCTGCAGAAGCTATGGAG-AAAGTCTTC and GAAGACTTTCTCCATAGCTTCTGC-AGACTTTTTTTCG for H105K. Single and triple histidine substitutions in the F107W background were overexpressed to produce the P protein variants used for this study. The DNA sequence and the mass spectrum of each variant were determined to ensure that it contained the desired substitution.

Wild-type P protein and variants were overexpressed in *Escherichia coli* [BL21 (DE3) pLysS] cells. For preparation of ^{15}N singly labeled and ^{15}N and ^{13}C doubly labeled protein used in the NMR experiments, a single colony of positive transformants was used to inoculate 30 mL of LB medium containing 50 μg/mL kanamycin and 17 μg/mL chloramphenicol and grown to an OD$_{600}$ of 0.8−0.9. The culture was diluted (1:200) into the M9 minimum medium culture (1 L) containing the same antibiotics and enriched with 2 g/L [^{13}C]glucose and/or 1 g/L [^{15}N]ammonium chloride. The culture was incubated until the OD$_{600}$ was 0.4−0.6 and protein overexpression induced by addition of IPTG to a final concentration of 0.4 mM. The culture was incubated with vigorous shaking (1 L in a 6 L Erlenmeyer flask) for 10−12 h, and the cells were harvested by centrifugation. Overexpressed P protein was purified as described previously (*33*) with the following modifications. The pooled fractions of P protein eluted from the second CM-Sepharose column were concentrated using a 3.5 kDa cutoff centriprep ultrafilter (Amicon) until the volume of the pooled fractions was reduced to 1−2 mL. The buffer in the sample was changed to 6 M guanidine hydrochloride (Gdn-HCl) with 10 mM Tris (pH 7.5) during this concentration step. The concentrated sample was then loaded on an S-100 column equilibrated with 6 M Gdn-HCl and 10 mM Tris (pH 7.5) to remove any bound EDTA. Fractions containing P protein were pooled and concentrated again using a centriprep ultrafilter to the desired concentration for NMR experiments. Protein purity was determined to be > 99% by SDS−PAGE with Coomassie blue detection. The molecular mass of each variant was confirmed by electrospray ionization mass spectrometry. The masses of unlabeled proteins were within 0.5 Da of the expected mass, and labeled proteins were 3−4 Da larger from the theoretical mass calculation. Protein was stored in 6 M Gdn-HCl at −80 °C for long-term storage. The protein NMR sample was dialyzed extensively against water and then 20 mM sodium cacodylate (with the proper pH value needed in the experiments). In all experiments, the protein concentration was calculated using the Edelhoch method (*34*) using an extinction coefficient of 5800 M^{-1} cm^{-1} and 11200 M^{-1} cm^{-1} at 276 nm for WT and F107W, respectively.

NMR Spectroscopy Experiments. (*i*) *Two- and Three-Dimensional NMR Experiments and Sequential Assignment.* All three-dimensional NMR spectra were recorded at 25 °C on a Varian INOVA 600 spectrometer with a triple-resonance cryoprobe equipped with a z-field gradient coil. The two-dimensional spectra were recorded on either a Varian INOVA 600 or a Varian INOVA 800 spectrometer with a triple-resonance probe. The NMR sample used for assignment of the extra peaks consisted of 0.5 mM P protein in 5 mM sodium sulfate, 20 mM sodium cacodylate buffer (pH 5.0), 10% D$_2$O, and 0.05% sodium azide. The NMR sample used for the pH titrations of the unliganded protein consisted of 0.2−0.4 mM P protein in 20 mM sodium cacodylate buffer, 10% D$_2$O, and 0.05% sodium azide. The pH ranged from 5 to 7.5. Two-dimensional gradient-enhanced

sensitivity-enhanced $^1H-^{15}N$ HSQC experiments were conducted with a spectral width in the ^1H dimension of 11990 Hz and 1024 complex points and a spectral width in the ^{15}N dimension of 1994 Hz and 192 complex points. The resonance assignments of extra peaks were made using a suite of triple-resonance experiments, including (HCA)CO(CA)NH (*35*), HNCO (*36*), HN(CA)CO (*37*), CBCA(CO)NH (*38*), and H(CCO)NH (*39*, *40*). In these three-dimensional NMR experiments, the spectral width in the ^1H dimension was 7020 Hz with 1024 complex points and the spectral width in the ^{15}N dimension was 1944 Hz with 32, 64, or 72 complex points. The spectral width in the ^{13}C dimension was 2000 Hz with 48, 64, and 96 complex points for (HCA)CO(CA)NH, HN(CA)CO, and HNCO, respectively. The spectral width in the ^{13}C dimension was 12066 Hz with 64 complex points for the CBCA(CO)NH experiment. The NMR spectra were processed using NMRpipe (*41*); the processed spectra were viewed and examined by NMRDraw and NMRviewJ, and the intensities of the cross-peaks were quantified with NMRViewJ (*42*). Backbone sequential assignments were analyzed using CARA (CARA can be downloaded for free from http://www.nmr.ch).

(*ii*) *Paramagnetic Relaxation Enhancement* (*PRE*) *Experiments*. Two-dimensional gradient-enhanced sensitivity-enhanced $^1H-^{15}N$ HSQC spectra were recorded on a Varian INOVA 600 spectrometer with a triple-resonance probe. The P protein concentration was 200 μM with 20 mM sulfate in 20 mM cacodylate buffer (pH 6.5), 10% D_2O, and 0.05% sodium azide. Potassium hexacyanochromate {$K_3[Cr(CN)_6]$} was titrated into the protein sample from 2.5 to 100 μM (with concentration steps of 5, 10, 20, and 50 μM). The HSQC spectra were recorded at each $[Cr(CN)_6]^{3-}$ concentration with a spectral width in the ^1H dimension of 7020 Hz and 1024 complex points and a spectral width in the ^{15}N dimension of 1994 Hz and 128 complex points.

RESULTS

Sulfate and pH Titration of Folded P Protein. Assignments for 95% of the backbone resonances of sulfate-folded (20 mM sulfate) P protein have been reported previously (*10*). Although most of the peaks present in the $^1H-^{15}N$ HSQC spectrum under these conditions were assigned in the previous studies, a few residues were missing and some extra peaks could not be assigned. One interpretation of these observations is that one or more alternative conformations are in chemical exchange with the folded state of P protein. In addition, the intensities of the extra peaks are dependent on ligand (sulfate) concentration and pH, suggesting that the population(s) of the alternative state(s) is influenced by ligand and pH. Sulfate has previously been shown to bind to P protein with an apparent affinity of 0.5 mM (*43*). To gain more insight into how ligand concentration and pH affect the equilibria between the alternative conformations and the folded state, a series of $^1H-^{15}N$ HSQC spectra were recorded at various sodium sulfate concentrations and pH values. The sulfate concentration ranged from 0 to 100 mM but focused on the range around 2−100 mM. As shown in Figure 1A, the intensities of the extra peaks decreased as the ligand concentration increased, and the chemical shifts of some assigned peaks of the folded state, many of which are in the N-terminal region, were strongly dependent on ligand concentration. These two observations indicate that both slow exchange and fast exchange processes contribute to the observed ligand dependence.

Similar effects were observed when the sample pH was varied. As shown in Figure 1B, the intensities of the unassigned extra
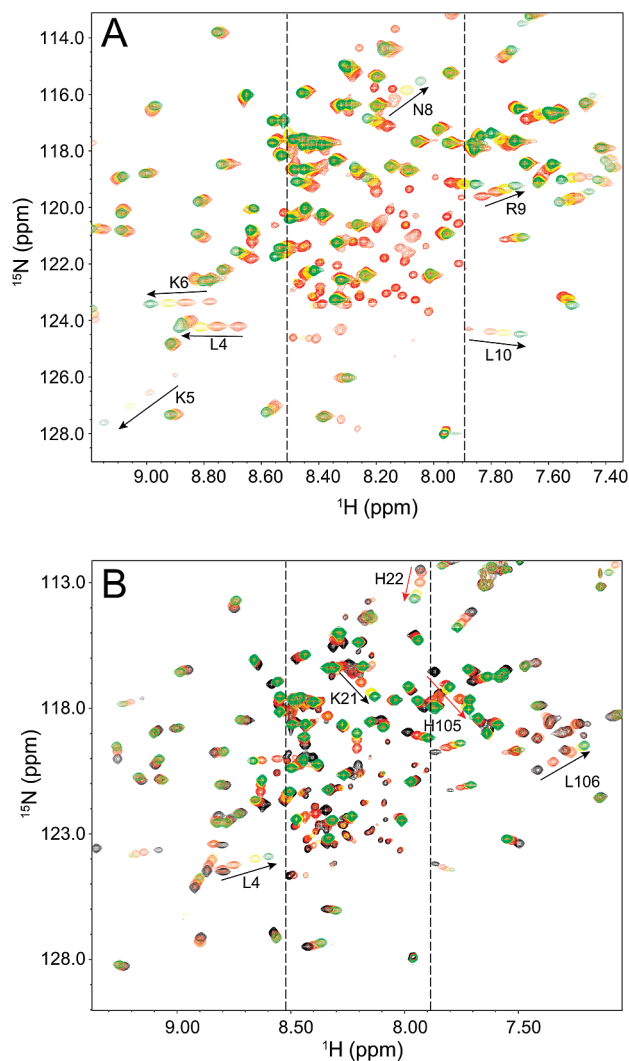

FIGURE 1: Sulfate titration and pH titration of the $^1H-^{15}N$ HSQC spectrum of ^{15}N-labeled P protein, at pH 6.0 and 25 °C. (A) The spectra of P protein in 5 (red), 10 (orange), 20 (yellow), and 100 mM sulfate (green) are overlaid in order of increasing concentration. The intensities of the extra peaks (between the two dashed lines) decrease with increasing sulfate concentrations as evidenced by the disappearance of the yellow and green peaks. The labeled peaks are assigned residues of folded P protein. The arrows show their change in frequency as the sulfate concentration increases from 5 to 100 mM. (B) The spectra of P protein in 20 mM sulfate at pH 5.3 (black), 5.5 (red), 6.0 (orange), 6.5 (yellow), and 7.0 (green) are overlaid in order of increasing pH. The labels for the two observable histidine residues are red. His 3 is not observed in the spectrum. Residues next to histidine residues that exhibit significant chemical shift movement are labeled in black, with arrows indicating their change in frequency with an increasing pH. All extra peaks are located in the region between the two dashed lines, and their intensities decrease with an increasing pH.

peaks decreased and many native peaks shifted as the sample pH was increased from 5.0 to 7.5 with the sulfate concentration held constant at 20 mM. The pK_a of the free histidine imidazole group is 6.0 (*44*), which is within the range of pH values used for this experiment. For this reason, it is likely that the changes in folded resonance frequencies can be explained by the change in the protonation state of the three histidine side chains in P protein. Figure 1B shows that the amide $^{15}N-^1H$ resonances assigned to His 22 and His 105 move as the pH changes, and the His 3 peak is missing in the spectrum, presumably because of intermediate chemical exchange (*10*). The ^1H or ^{15}N chemical shifts of the two
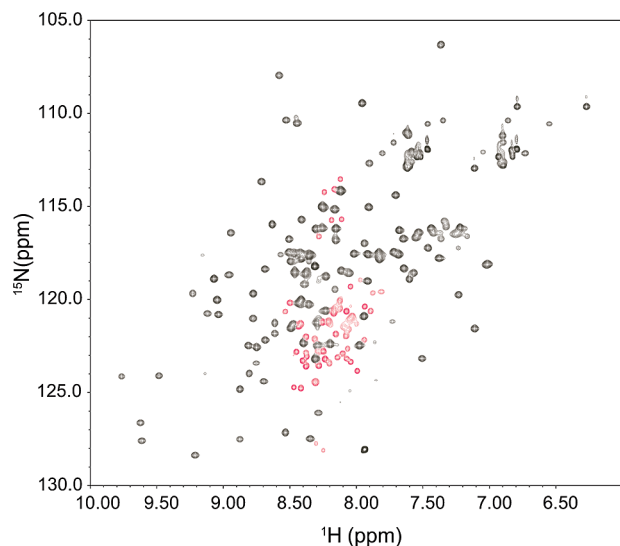
FIGURE 2: $^1H-^{15}N$ HSQC spectrum of ^{15}N-labeled P protein in 5 mM sulfate at pH 5.0 and 25 °C. The gray peaks are the folded state spectrum resonances assigned in a previous study (*56*). The red peaks are extra peaks that appear under these buffer conditions. All of the extra peaks are located between 7.9 and 8.5 ppm in the ^1H dimension. The assignment results of the extra peaks are listed in the Supporting Information.

FIGURE 3: $^1H-^{15}N$ HSQC spectrum of ^{15}N-labeled P protein in 20 mM sodium cacodylate at pH 5.0 and 25 °C. Sulfate is not present in the sample, so P protein is predominantly unfolded. The peaks in the spectrum are poorly dispersed compared to those of the folded P protein spectrum in Figure 1. The peaks in the two circles form patterns similar to those found in the folded P protein spectrum. The intensities of these peaks are weaker than those of the remaining unassigned resonances from unfolded P protein. The two insets show the overlapped HSQC spectra of unfolded (black) and folded P protein (red) in the circled regions. Labeled peaks are previously assigned to residues in folded P protein.

histidine resonances plotted versus pH can be fitted to the Henderson−Hasselbalch equation to estimate the pK_a values of His 22 and His 105, which are 6.08 ± 0.16 and 5.65 ± 0.17, respectively (Supporting Information). Changes in chemical shift were also observed for residues in the proximity of all three histidine residues, which is expected because the ionization state of the histidine side chain can also affect neighboring residues.

HSQC Spectrum of Folded P Protein and Unfolded P Protein. In a previous study (*10*), the protein sample conditions (pH 6.0 and 20 mM sodium sulfate) reduced the intensity of the extra peaks, producing an HSQC spectrum dominated by folded P protein resonances. However, as described in the previous section, lowering the sulfate concentration to 5 mM and decreasing the sample pH from 6.0 to 5.0 increase the intensities of the unassigned extra peaks. As shown in Figure 2, there are approximately 50 unassigned peaks (colored red) present in the spectrum, and most of them are located in the 8.0 to 8.5 ppm region of the ^1H spectrum. The presence of extra peaks means that some residues in the folded P protein produce two (or multiple) cross-peaks in the HSQC spectrum. Therefore, the residues in P protein can be classified into three types. Residues that have only one peak are in fast exchange ($\Delta\omega \ll k$) between the alternative and folded states. In the limit, $\Delta\omega$ is equal to 0, implying that the magnetic environments of those residues in the alternative and folded states are similar or even the same. Residues that produce no detectable HSQC resonances presumably correspond to sites in intermediate exchange ($\Delta\omega \cong k$) between the different conformational states. The sensitivity of the INEPT coherence transfer steps in the HSQC pulse sequence to chemical exchange processes (*45*) and severe line broadening (*46*) both contribute to a severe loss of peak intensity in this regime. Residues that can be assigned to two peaks correspond to sites in slow exchange ($\Delta\omega \gg k$) between the alternative and folded states. The large difference in frequency indicates that these residues are found in quite different magnetic environments in the alternative and folded states.

Figure 3 shows the HSQC spectrum of P protein at the same pH values used for Figure 2, but in the absence of sulfate. Under
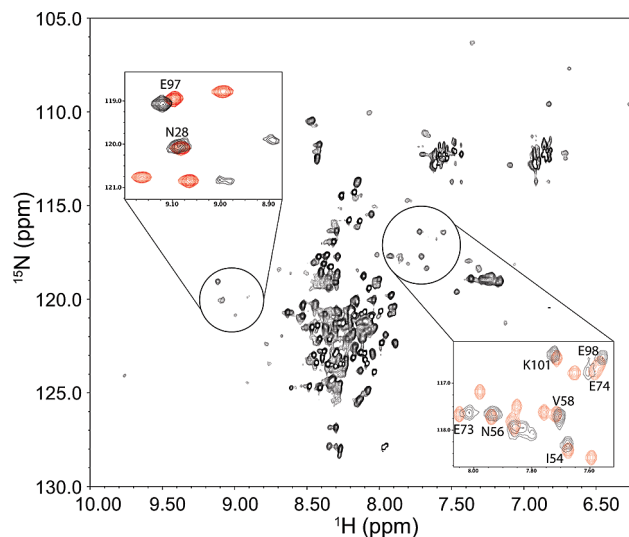
these conditions, the protein is predominantly unfolded. This spectrum is characteristic of unfolded polypeptides, but there are two subsets of peaks (circled regions) whose positions are similar to those of assigned resonances in the HSQC spectrum of sulfate-folded P protein (*10*). As shown in Figure 3, the peaks in these circled regions overlapped well between the unfolded and folded conditions, which is strong evidence that these peaks correspond to the same residues in the protein. The presence of assigned peaks of folded P protein in the unfolded P protein spectrum can be explained by the presence of a partially folded species that exchanges slowly ($\tau_{ex} > 1$ s) with the fully unfolded protein. The presence of extra peaks and missing residues in the sulfate-folded state spectrum is evidence of the existence of one (or more) alternative conformation that exchanges slowly with the folded conformation. Taken together, both HSQC spectra are consistent with the presence of an alternative structural conformation that is in equilibrium between the unfolded and folded state. This interpretation is supported by our folding kinetic studies of P protein, which demonstrated that there is an intermediate state in the P protein folding process (*12*). Although our previous kinetic and equilibrium studies (*12*) of TMAO-folded protein did not involve ligand binding, similar studies of ligand induced folding also show the presence of an intermediate species in the folding process (unpublished data). Therefore, as a minimal complexity model that is consistent with all of the experimental data, we have assigned the alternative conformation found in the NMR spectra collected under both folding and unfolding conditions to the same partially folded intermediate state in the P protein folding mechanism. Assignment of the extra peaks in the HSQC spectrum (Figure 2) allowed identification of residues in the unfolded regions of the partially sulfate-folded intermediate.

Assignment of Extra Peaks in the Folded P Protein HSQC Spectrum. To assign the extra peaks, a protein sample in 5 mM sodium sulfate (pH 5.0) was chosen to intensify the extra
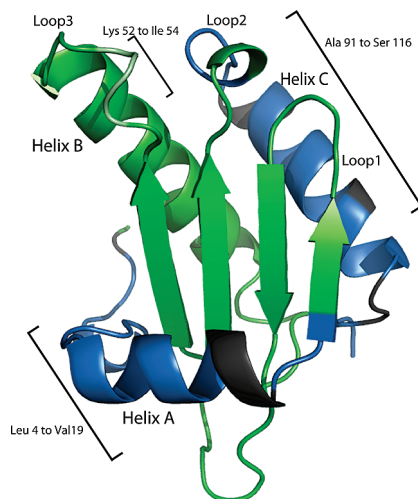
FIGURE 4: Mapping of the residues assigned to extra HSQC resonances on the crystal structure of folded P protein. The residues colored blue are the extra peaks that are assigned in the study. The residues colored dark gray are the residues that might have the extra peaks but could not be unambiguously assigned. The remaining residues colored green have a single resonance in the spectrum.

FIGURE 5: Chemical shift analysis of the extra peaks in the folded P protein HSQC spectrum. Data for residues 52−54 are colored light green because their CSI values are larger than 2 ppm.

peaks. Standard multidimensional backbone assignment experiments with ^{13}C- and ^{15}N-labeled protein were performed, and a total of 50 extra peaks were observed in the HSQC spectrum. The clustering of the peaks in the 8−8.5 ppm ^{1}H chemical shift range resulted in partial overlap of many of the extra peaks. This problem, combined with the relatively weak intensities of the extra peaks, made their assignments more challenging to determine than those of the folded resonances. Combination of data from HNCO (36), HN(CA)CO (37), and (HCA)CO(CA)NH (35) experiments allowed the sequential assignments through the ^{13}CO nuclei. The HNCACB (47) and CBCA(CO)NH (38) experiments were also included to detect ^{13}C$_\alpha$ and ^{13}C$_\beta$ resonance, and the results further aid and validate the ^{13}CO assignment. There were some short stretches consisting of three to five residues that could not be unambiguously assigned to definite fragments in the protein sequence. To resolve this ambiguity, an H(CCO)NH (39, 40) three-dimensional experiment was performed to detect the side chain proton spin system of residue $i − 1$, and subsequently, each fragment was assigned to its correct sequence. This suite of experiments allowed for the assignment of 42 of the 50 observed extra peaks. Five of the remaining eight peaks exhibited no ^{13}C chemical shift connectivity to each other or any of the peaks of the folded state. The chemical shifts for the backbone atoms of the 42 assigned peaks and the eight unassigned peaks can be found in the Supporting Information.

Most of the extra peaks were assigned to residues located near the N- and C-termini in the protein sequence. There is one long N-terminal fragment from Leu 4 to Val 19, which is halfway through helix A in the folded structure (Figure 4). Four short fragments (Ala 91−Thr 95, Glu 98−Gln 104, Leu 106−Arg 109, and Leu 112−Ser 116) are located in the C-terminal region, which includes loop 2 and most of helix C. A short fragment from Lys 52 to Ile 54 is located outside of these two structural regions. Inspection of the chemical shifts listed in Table S1 of the Supporting Information indicates that many extra peaks assigned to the same residue type are clustered near each other in the HSQC spectrum, which suggests that these residues are located in a highly solvated magnetic environment in the intermediate.
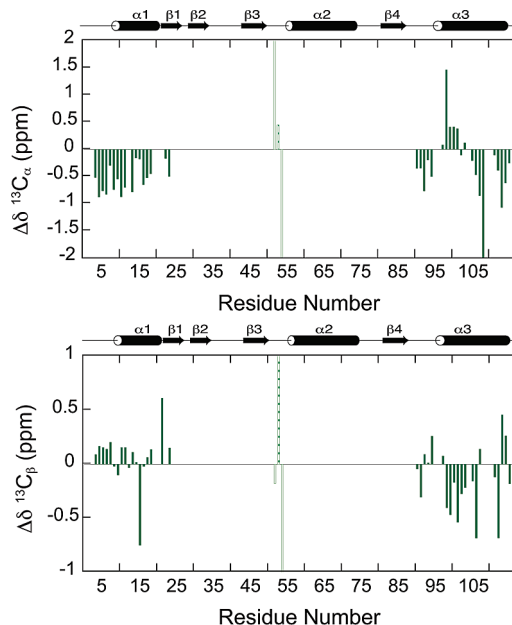
Chemical shift indices (CSIs) for ^{13}C$_\alpha$ and ^{13}C$_\beta$ assignments can be used to deduce secondary structure from established empirical relationships (48, 49). ^{13}C$_\alpha$ resonances experience a downfield shift relative to random-coil shifts in α-helical conformations, and the ^{13}C$_\alpha$ chemical shift is typically upfield of random-coil shifts when the residue is in a β-strand conformation. The chemical shift index values as a function of protein sequence for ^{13}C$_\alpha$ and ^{13}C$_\beta$ atoms of the extra peaks are shown in Figure 5. The N-terminal region of folded P protein is a flexible structure followed by helix A to residue S25. Most of the ^{13}C$_\alpha$ CSI values of the stretch of 18 assigned extra peaks in this region are smaller than 1 ppm, and there is no significant deviation from random-coil shifts, indicating that these residues have a random-coil-like structure in the intermediate state. Extra peaks assigned to residues found in the C-terminal helix C region of the folded state have ^{13}C$_\alpha$ CSI values indicative of random coil, supporting the conclusion that this region of the intermediate state is also unfolded. The ^{13}C$_\beta$ CSI values are consistent with these conclusions. For the extra peaks assigned to these two regions, the differences in chemical shifts from the folded state assignments are greater than 3 ppm. The three residues in the middle of the sequence in Figure 5 are colored light green to indicate that their CSI values are not consistent between ^{13}C$_\alpha$ and ^{13}C$_\beta$, and some of them are larger than 2 ppm. Low chemical shift dispersion of the extra peak ^{1}H−^{15}N HSQC resonances and their low ^{13}C$_\alpha$ and ^{13}C$_\beta$ CSI values are consistent with the conclusion that these residues are unfolded in the partially folded intermediate. In addition, TALOS+ (50) uses available chemical shifts (H$_\alpha$, HN, H, C$_\alpha$, C$_\beta$, and CO) to calculate a random-coil index (RCI) and predict the secondary structure. The secondary structure prediction from TALOS+ is consistent with CSI values. The order parameter (S^2) prediction from the program shows these regions are dynamic ($S^2 < 0.5$), which agrees with the fact that these residues are in the unfolded state.

Effect of Histidine Replacement in P Protein. As shown in Figure 3, the presence of assigned peaks of the folded state in the unfolded P protein spectrum can be explained by the presence of
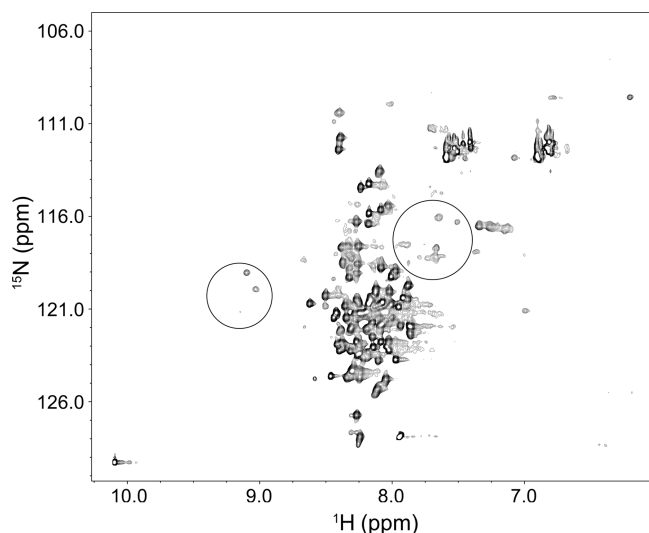
FIGURE 6: $^1H-^{15}N$ HSQC spectrum of the ^{15}N-labeled F107W variant of P protein in 20 mM sodium cacodylate at pH 6.0 and 25 °C. The peaks in the spectrum are as poorly dispersed as those of unfolded WT P protein shown in Figure 3. The peaks in the two circles are assigned folded state P protein residues also present in the unfolded P protein spectrum. The intensities of these peaks are weaker than those of the remaining unassigned peaks of unfolded P protein.

the intermediate state, which exchanges slowly with the unfolded state. To investigate how the histidine residues in the protein perturb the equilibrium between the U and I states, we constructed different single His to Lys variants (H3K, H22K, and H105K) and a triple His to Lys variant (HtriK) to study the effects. These variants were made in the background of the F107W variant to allow both NMR and fluorescence stopped-flow experiments. Because the F107W substitution has little effect on the overall structure and stability of P protein, the $^1H-^{15}N$ HSQC spectrum of unfolded F107W is similar to that of the wild type (WT), including the peaks of the folded state observed in the unfolded WT spectrum (circled area in Figure 6). A series of pH titration experiments from pH 5.0 to 7.0 monitored by HSQC spectra were performed to investigate the effect of pH on the equilibrium between the U and I states. As shown in Figure 7A, when the pH is increased from 5.0 to 7.0, the intensities of the foldedlike peaks due to I also increase. This means that the relative population of I increases as the pH increases. These results suggest that the ionization of histidine residues in the P protein affects the equilibrium transition between U and I, because the histidine side chain is the only likely titratable group in this pH range. The HtriK variant was constructed to mimic the charge state of the F107W variant at pH 5.0, because the histidines are more than 80% protonated (>93% for His 22 and >82% for His 105) and carry a positive charge at that pH. As shown in Figure 7B, the HtriK substitutions almost completely abolish the intensities of the peaks of the folded state in the HSQC spectrum, which is now independent of pH. This is the expected result if the extra charge on the variant depopulates I. Because P protein is a highly basic protein containing 19 Lys and 11 Arg residues, introducing three more Lys residues into the protein increases the level of electrostatic repulsion in the fully or partially folded forms, favoring the unfolded state of the protein.

Subsequent pH titration experiments were performed on each single H → K variant to determine which histidine residue(s) accounts for the observed effects. As shown in Figure 7C−E, the
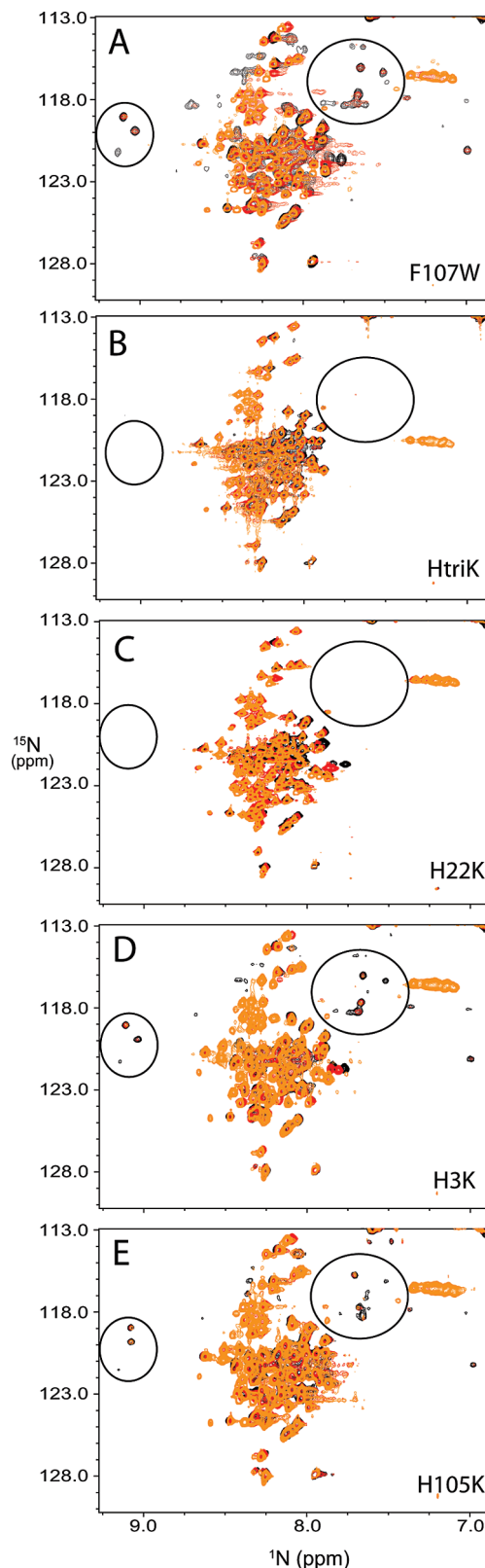

FIGURE 7: HSQC spectra of various histidine variants of P protein under unfolding conditions at three pH values. The pH titration experiments were conducted at pH 5.0 (orange), 6.0 (red), and 7.0 (black) for each variant. The name of the variant is in the bottom right corner of each plot. The spectra are overlaid, and the peaks in the circled area are assigned peaks of the folded state of F107W. As shown in the plots, the intensities of the peaks in the circled area increase as the pH increases.

HSQC spectrum of the H22K variant is nearly the same as that of the HtriK variant, suggesting that protonation of this histidine,

located at the end of helix A, is the source of the pH dependence of the U−I equilibrium. The spectrum of H105K shows a pH dependence similar to that of F107W, indicating that the protonation of His 105 has little effect on the stability of I. The pH dependence of peak intensities in the H3K variant spectrum shows that His 3 does have an effect on the population of I, but the effect is smaller than that of His 22.

On the basis of the pH titration experiments performed with these different variants, we conclude that as the pH is increased from 5 to 7, the equilibrium between U and I is shifted toward I primarily by the deprotonation of His 22, with some contribution from His 3 and little or none from His 105.

Identification of Ligand Binding Sites by PRE. Our previous studies showed that the stoichiometry of binding of an anion to P protein is 2 and proposed the locations of the two high-affinity binding sites responsible for the folding-coupled binding transition of P protein (*43*). The electron density of one sulfate was clearly observed by X-ray crystallography near the N-terminus, with sulfate coordinated by His 3, Arg 9, and Arg 68 (*51*). We later proposed that the second site is located near Arg 88 and Lys 89, although Stams et al. had assigned the observed electron density at that site to a water molecule instead of a sulfate ion. To identify the anion binding sites more definitively, we used paramagnetic relaxation enhancement (PRE) NMR experiments. PRE is caused by magnetic dipole interactions between a nucleus and the unpaired electrons (*52*) and results in an increase in the relaxation rate of the nuclear magnetization. Its magnitude is proportional to $\langle r^{-6} \rangle$ (where r is the distance between the nucleus of interest and the paramagnetic center) (*53*). As a result of the large magnetic moment of an unpaired electron, the effect of the PRE can be detected at a fairly long range (15−24 Å). Previous studies used the paramagnetic hexacyanochromate-(III) ion $\{[Cr(CN)_6]^{3-}\}$ to probe the active site of RNase A (*54*) and the anion binding site of phosphoglycerate kinase (*55*). We have used the same anion for the PRE studies of the P protein anion binding site.

The apparent affinity of P protein for $[Cr(CN)_6]^{3-}$ was determined by CD-detected titration, with this ligand yielding an apparent K_d of approximately 20 μM (data not shown), consistent with the high-affinity binding expected for a trivalent anion. Subsequently, $[Cr(CN)_6]^{3-}$ titration experiments monitored via the $^1H-^{15}N$ HSQC spectrum were performed to identify the P protein residues in the proximity of the anion binding sites. The initial NMR sample contained 200 μM folded P protein in 20 mM sulfate (pH 6.5). $[Cr(CN)_6]^{3-}$ was added to the sample at concentrations ranging from 2.5 to 100 μM. Because $[Cr(CN)_6]^{3-}$ is more tightly bound than sulfate, 2.5 μM $[Cr(CN)_6]^{3-}$ was sufficient to displace some of the bound sulfate. It is also reasonable to assume that the on rates of the paramagnetic ligand are diffusion-limited (at least 10^6 M^{-1} s^{-1}). Under these conditions, there would be at least 20 $[Cr(CN)_6]^{3-}$ binding events within the T_1 of the ^1H or ^{15}N spins. Thus, even if the population of the sites with $[Cr(CN)_6]^{3-}$ is small (<1%), this minor species can still strongly affect the apparent relaxation rate and cause line broadening of the $^1H-^{15}N$ HSQC resonances from the backbone amides of nearby residues. Figure 8 shows HSQC spectra from the $[Cr(CN)_6]^{3-}$ titration experiments. With the addition of the $[Cr(CN)_6]^{3-}$ ion, the amide peak intensities of the residues that are in vicinity of the binding sites start to decrease or completely broaden out. These residues are labeled in Figure 8. The degree of the intensity decrease of a residue as a function of $[Cr(CN)_6]^{3-}$ concentration provides information about the distance between the amide and the paramagnetic center. The
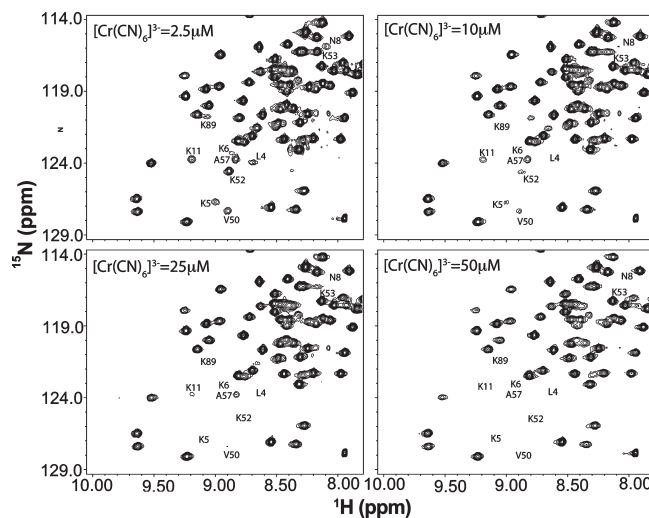

FIGURE 8: $^1H-^{15}N$ HSQC spectrum of folded P protein in various concentrations of $K_3[Cr(CN)_6]$. The protein concentration was 200 μM with 20 mM sulfate in 20 mM cacodylate buffer (pH 6.5). The $[Cr(CN)_6]^{3-}$ concentration ranged from 2.5 to 50 μM. The spectra at $[Cr(CN)_6]^{3-}$ concentrations of >50 μM are not shown in the plot. Higher concentrations of $[Cr(CN)_6]^{3-}$ broaden the resonances of many residues, which may result from nonspecific binding of $[Cr(CN)_6]^{3-}$, thereby masking the effects due binding at the two high-affinity sites.
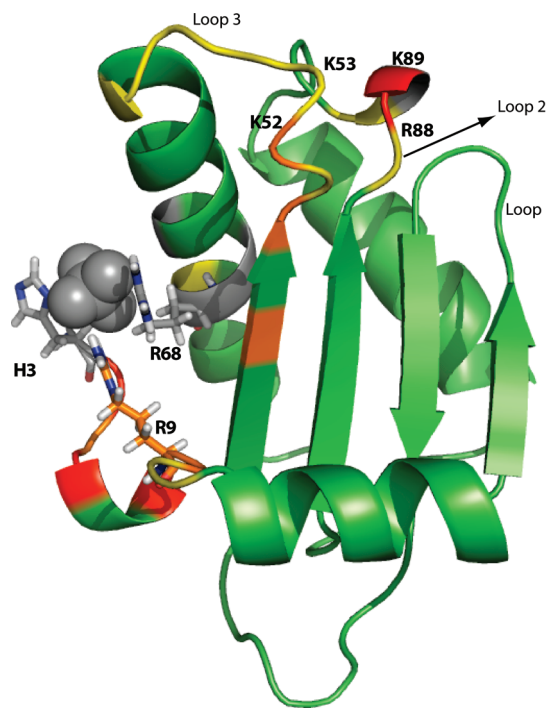

FIGURE 9: PRE results mapped on the P protein crystal structure. The results of the NMR PRE experiments show two regions of P protein involved in the anion binding. The color of each residue indicates the $[Cr(CN)_6]^{3-}$ concentration at which the associated resonance intensity is affected: red for 2.5 μM, orange for 5−10 μM, and yellow for 25−50 μM. Residues colored gray correspond to resonances already missing in the 0 M $[Cr(CN)_6]^{3-}$ HSQC spectrum, prolines, or unresolved peaks. Residues colored green are unaffected by $[Cr(CN)_6]^{3-}$ between 2.5 and 100 μM.

lower the $[Cr(CN)_6]^{3-}$ concentration needed to broaden the peak, the closer the residue is to the binding site. As seen in Figure 9, mapping the affected residues to the structure of the P protein identified two anion binding sites as expected. In general, the PRE NMR results agree with the previously proposed anion binding

sites, especially the one located in the N-terminal region. The other site is also close to the previously proposed site, but Lys 89 and Lys 52 amide resonances were more strongly affected by the paramagnetic anion than the Arg 88 amide. This suggests that the second anion binding site might be close to the loop 2 and loop 3 regions indicated in Figure 9, rather than the loop 1 and loop 2 region as previously proposed (*43*).

DISCUSSION

Structural Description of the Intermediate State. Figure 4 shows the residues assigned to the extra peaks present in the folded P protein ^{1}H$-^{15}$N HSQC spectrum mapped on the crystal structure of P protein. The extra peak residues are colored blue on the structure, and most are located in the N-terminal (residues 3−19) and C-terminal (residues 91−116) regions. Three of the extra peaks were assigned to Lys 52−Ile 54, which are located in the middle of loop 3. The low chemical shift dispersion of the extra ^{1}H$-^{15}$N HSQC resonances and their low ^{13}C$_\alpha$ and ^{13}C$_\beta$ CSI values indicate that the associated residues are part of the random-coil-like structure in I. It should be noted that each of the assigned residues in these three regions has two separate cross-peaks in the HSQC spectrum. One peak corresponds to the folded state resonance assigned in previous studies (*10, 56*), and the other corresponds to a resonance whose magnetic environment appears to be very similar to that of an unfolded protein. No extra peaks were assigned to the residues colored green in Figure 4, suggesting that these residues retain a foldedlike magnetic environment in both the intermediate and folded states. The residues colored dark gray in Figure 4 (Phe 20, Lys 21, His 22, Tyr 96, Glu 97, His 105, Ser 110, and Ser 111) are near the N- and C-termini but cannot be unambiguously assigned to any of the extra peaks. Residues unfolded in I would not have an extra peak if the differences between their folded and unfolded frequencies are small, i.e., if their folded state frequencies happen to be near the random-coil values. This might be the case for residues 20−22, 105, 110, and 111, because their folded state ^{1}H chemical shifts are between 8 and 8.5 ppm, near the random-coil values. This explanation, however, is not valid for Tyr 96 and Glu 97, because their ^{1}H chemical shifts are downfield at 9.7 and 9.5 ppm, respectively. An alternative explanation could be that because only 42 of 50 extra peaks have been assigned, the eight remaining unassigned peaks might correspond to these residues. The intensities of these unassigned peaks are weakest among the extra peaks in the HSQC spectrum, and they correspond to even weaker or missing cross-peaks in the three-dimensional heteronuclear triple-resonance experiments. Therefore, it was difficult to obtain sequential assignments for these eight peaks. An ideal solution would be assignment of the spectrum of completely unfolded P protein allowing the identification of the remaining unassigned peaks. The last possibility is that these eight peaks belong to residues outside the N- and C-terminal regions and could be some of the residues colored dark green in Figure 4. On the basis of the results of the NMR experiments, the likely structure of the intermediate includes a foldedlike central β-sheet and α-helix B with the N-terminal region through helix A and the C-terminal helix C unfolded.

Reconsideration of Previous Dynamic and Amide−Hydrogen Exchange Data. Previous backbone dynamics studies of P protein demonstrated the conformational heterogeneity of P protein under sulfate-folded conditions. A significant R_{ex}, the conformational exchange contribution of R_2, was found for some residues in

N- and C-terminal regions. These are the same regions that are unfolded in the intermediate state. On this basis, we propose that the previously observed R_{ex} values might be due to the folding and unfolding of helix A and helix C to form I under conditions that mostly populate the folded protein. Some residues in the RNR motif of P protein exhibit significant R_{ex} values but are not unfolded in the intermediate conformation we propose. These could correspond to the eight unassigned extra peaks in the HSQC spectrum.

Our previous studies have shown that there are two anion binding sites in P protein (*43*). In principle, each state (U, I, and N) can bind either one or two ligands (L) (e.g., IL, IL$_2$, NL, and NL$_2$). Hydrogen exchange (HX) studies showed that the ligand concentration could highly perturb the exchange pathway (*56*). In the presence of 20 mM sulfate, the primary routes of HX are principally through N and NL (singly liganded folded state). In 200 mM sulfate, the primary routes of HX change and are through NL and NL$_2$ states. However, in this previous exchange scheme, the intermediate state was not included in the analysis. If the intermediate state is taken into account, it is very likely that the HX from I or IL (singly liganded I) is more significant than the HX from N and NL. This mechanism may be particularly dominant at low ligand concentrations, because the population of IL is significant at 20 mM sulfate (the population of I with IL and IL$_2$ is ∼5% of the total protein). Under the experimental conditions used to assign the extra peaks (5 mM sulfate), the total population of I is ∼10% of the total protein (unpublished). Therefore, the intermediate state likely plays a major role in the HX pathway of P protein. Because our previous studies did not recognize the existence of an intermediate, the mechanisms of exchange presented were probably incomplete.

Unstructured N- and C-Termini of I May Fold Independently to N. As shown in Figure 4, α-helix A and α-helix C are spatially separated from each other. It is possible that the two α-helices fold independently, which would lead to three intermediate states: both helices unfolded, helix A unfolded, and helix B unfolded. There are some hints in the data that this might be the case. As shown in Figure 1A, as additional sulfate is added to P protein all the extra peaks disappear at roughly the same sulfate concentration. However, a more detailed comparison of the extra peaks from the N- and C-termini indicates that the C-terminal residues completely disappear between 10 and 20 mM, and N-terminal residues completely disappear above 20 mM. In addition, the HSQC peaks in the folded state spectrum that appear to correspond to the peaks in the unfolded state spectrum were previously assigned to residues Glu 97, Glu 98, and Lys 101 (circled regions in Figure 3). These residues are close to the C-terminal helix and are observed as extra peaks in the sulfate-folded spectrum. Thus, the population of intermediate species with helix A unfolded and helix C folded appears to exceed that of the other two intermediate species under some conditions. The kinetic mechanism developed in our previous kinetic studies (*12*) of P protein is the simplest mechanistic model consistent with the experimental data. If the folding rate constants of N-terminal and C-terminal helices are similar to each other, the kinetic experiments would be unable to distinguish multiple intermediate conformations. For this reason, we will still treat I as a single thermodynamic state with incompletely characterized conformational heterogeneity.

Effect of Histidine Ionization on Conformational Equilibria. The results of the pH titration of the various H → K variants indicate that ionization of both His 3 and His 22 perturbs the relative populations of U and I between pH 5.0 and 7.0 and

His 22 has a major effect on this equilibrium. Because only three different pH values were examined for each variant, the NMR experiments provide only qualitative information about the effect of histidine ionization on the stability of U and I. As shown in Figures 3 and 7, the effect of increasing pH (i.e., deprotonating the histidines) is to shift the I−N conformational equilibrium toward N in the presence of sulfate and the U−I equilibrium toward I in the absence of sulfate. These effects likely arise from unfavorable electrostatic interactions in more compact forms of the protein. At pH 5.0 in the absence of sulfate, the repulsive forces due to additional net positive charge from the protonated histidine residues presumably increase the free energy of I relative to that of the less compact U, so P protein favors the U state. When the pH is increased, the neutralization of the histidines relieves some repulsive forces and lowers the free energy of I relative to U. The same principle can be used to explain the effect of pH on the I−N equilibrium in the presence of sulfate.

To obtain more quantitative estimates of the effect of pH on U, I, and N free energies in F107W and the histidine variants, a more finely stepped pH titration followed by NMR is necessary. The relative populations of U and I could be estimated as a function of pH using the relative peak intensities in the HSQC spectrum for each variant. In addition, the chemical shifts of the $^{13}C_2$-^1H spin pair in selectively labeled His side chains would provide a sensitive probe for the pK_a of each. Thermodynamic coupling between His proton binding and protein conformational change would allow quantitative estimation of the energetic contributions of electrostatic interactions in conformational equilibria.

Ligand Interactions and Biological Relevance of the Intermediate State. The results of the PRE NMR experiments, summarized in Figure 9, showed good agreement with the previously modeled binding sites in the P protein (*43*). Leu 4, Lys 6, and Arg 9 in the N-terminal region are strongly affected by the paramagnetic anions, indicating that they are in the proximity of the sulfate binding site (formed by the His 3, Arg 9, and Arg 68 side chains) observed in the crystal structure (*51*). The cross-peak of His 3 is missing in the ^1H−^{15}N HSQC spectrum, and the cross-peak of Arg 68 is overlapped with other two strong peaks, Ser 116 and Ser 117. For these reasons, the PRE of H3 and R68 could not be determined, and they are accordingly colored gray in Figure 9. The second binding region probed by paramagnetic anion is also close to the previously proposed region (*43*), based on excess electron density observed in water 108 in the crystal structure (*51*). Interestingly, Lys 89 (colored red) is affected most strongly by the paramagnetic anion, followed by Lys 52 (colored orange). Arg 88 (colored yellow) is actually less affected than either Lys 89 or Lys 52. These results point out some discrepancies between the crystal structure shown in Figure 9 and the PRE NMR data. In the crystal structure, the amide group of Lys 53 is closer to that of Lys 89 than to the Lys 52 amide. However, the peak intensity of Lys 52 is broadened out at lower concentrations of the paramagnetic anion compared to that of Lys 53, indicating that the amide group of Lys 52 is closer to Lys 89. The loop region between residues 51 and 60 has the highest *B* factor values in the crystal structure, suggesting that the loop has significant flexibility (*51*). The loop orientation observed in the crystal structure may be one of several conformations of this region present in solution. On the basis of the PRE NMR experiments, we conclude that Lys 89 and Lys 52 likely play an important role in forming the second anion binding site of P protein.

On the basis of our proposed structure of the intermediate state, only one high-affinity anion binding site would be present in the forms of the intermediate lacking the N-terminal helix. This conclusion is supported by our ligand-induced folding kinetics data (manuscript in preparation), which suggests that one anion ligand binds with much higher affinity to the partially folded intermediate than the other. Interestingly, the majority of helix B and the central β-sheet are formed in the intermediate state. Helix B contains the conserved RNR motif in the P protein and has many crucial contacts with P RNA (*57*). The central β-sheet also has many interactions with the pre-tRNA leading sequence during catalysis (*58, 59*). Given the preservation of the structural elements key to RNA interactions in the intermediate state, these regions may represent the functional core of the protein and may be key to the holoenzyme assembly process. Moreover, the population of I under physiological conditions that is surrounded by different anions will also be important to the process. Future mechanistic studies of holoenzyme assembly will be aimed at delineating the role of the partially folded intermediate ensemble in this process.

SUPPORTING INFORMATION AVAILABLE

Chemical shifts of backbone NH, N, CO, C_α, and C_β atoms of the extra peaks in the folded P protein spectra (Table S1) and titration curves of His 22 and His 105 between pH 5 and 8 monitored by nitrogen chemical shifts from ^{15}N HSQC spectra (Figure S1). This material is available free of charge via the Internet at http://pubs.acs.org.

REFERENCES

1. Teilum, K., Maki, K., Kragelund, B. B., Poulsen, F. M., and Roder, H. (2002) Early kinetic intermediate in the folding of acyl-CoA binding protein detected by fluorescence labeling and ultrarapid mixing. *Proc. Natl. Acad. Sci. U.S.A. 99*, 9807–9812.
2. Capaldi, A. P., Shastry, M. C., Kleanthous, C., Roder, H., and Radford, S. E. (2001) Ultrarapid mixing experiments reveal that Im7 folds via an on-pathway intermediate. *Nat. Struct. Biol. 8*, 68–72.
3. Sánchez, I., and Kiefhaber, T. (2003) Evidence for sequential barriers and obligatory intermediates in apparent two-state protein folding. *J. Mol. Biol. 325*, 367–376.
4. Clark, A. C. (2008) Protein folding: Are we there yet? *Arch. Biochem. Biophys. 469*, 1–3.
5. Krantz, B. A., Mayne, L., Rumbley, J., Englander, S. W., and Sosnick, T. R. (2002) Fast and slow intermediate accumulation and the initial barrier mechanism in protein folding. *J. Mol. Biol. 324*, 359–371.
6. Fersht, A. R. (1995) Optimization of rates of protein folding: The nucleation-condensation mechanism and its implications. *Proc. Natl. Acad. Sci. U.S.A. 92*, 10869–10873.
7. Deka, P., Rajan, P. K., Perez-Canadillas, J. M., and Varani, G. (2005) Protein and RNA dynamics play key roles in determining the specific recognition of GU-rich polyadenylation regulatory elements by human Cstf-64 protein. *J. Mol. Biol. 347*, 719–733.
8. Shajani, Z., and Varani, G. (2005) ^{13}C NMR relaxation studies of RNA base and ribose nuclei reveal a complex pattern of motions in the RNA binding site for human U1A protein. *J. Mol. Biol. 349*, 699–715.
9. Mittermaier, A., Varani, L., Muhandiram, D. R., Kay, L. E., and Varani, G. (1999) Changes in side-chain and backbone dynamics identify determinants of specificity in RNA recognition by human U1A protein. *J. Mol. Biol. 294*, 967–979.
10. Henkels, C. H. (2005) Biophysical studies of *Bacillus subtilis* ribonuclease P protein. pp xi, 303 leaves, Duke University, Durham, NC.
11. Henkels, C. H., Chang, Y.-C., Chamberlin, S. I., and Oas, T. G. (2007) Dynamics of backbone conformational heterogeneity in *Bacillus subtilis* ribonuclease P protein. *Biochemistry 46*, 15062–15075.
12. Chang, Y.-C., and Oas, T. G. (2010) Osmolyte-Induced Folding of an Intrinsically Disordered Protein: Folding Mechanism in the Absence of Ligand. *Biochemistry 49*, 5086–5096.

13. Williamson, J. (2000) Induced fit in RNA-protein recognition. *Nat. Struct. Biol. 7*, 834–837.

14. Weeks, K. (1997) Protein-facilitated RNA folding. *Curr. Opin. Struct. Biol. 7*, 336–342.

15. Maity, T. S., and Weeks, K. M. (2007) A threefold RNA-protein interface in the signal recognition particle gates native complex assembly. *J. Mol. Biol. 369*, 512–524.

16. Roder, H., and Colón, W. (1997) Kinetic role of early intermediates in protein folding. *Curr. Opin. Struct. Biol. 7*, 15–28.

17. Baldwin, R. L. (1996) On-pathway versus off-pathway folding intermediates. *Folding Des. 1*, R1–R8.

18. Maki, K., Cheng, H., Dolgikh, D. A., and Roder, H. (2007) Folding kinetics of staphylococcal nuclease studied by tryptophan engineering and rapid mixing methods. *J. Mol. Biol. 368*, 244–255.

19. Shastry, M. C., Luck, S. D., and Roder, H. (1998) A continuous-flow capillary mixing method to monitor reactions on the microsecond time scale. *Biophys. J. 74*, 2714–2721.

20. Mayor, U., Johnson, C. M., Daggett, V., and Fersht, A. R. (2000) Protein folding and unfolding in microseconds to nanoseconds by experiment and simulation. *Proc. Natl. Acad. Sci. U.S.A. 97*, 13518–13522.

21. Park, S. H., Shastry, M. C., and Roder, H. (1999) Folding dynamics of the B1 domain of protein G explored by ultrarapid mixing. *Nat. Struct. Biol. 6*, 943–947.

22. Korzhnev, D. M., Neudecker, P., Mittermaier, A., Orekhov, V. Y., and Kay, L. E. (2005) Multiple-site exchange in proteins studied with a suite of six NMR relaxation dispersion experiments: An application to the folding of a Fyn SH3 domain mutant. *J. Am. Chem. Soc. 127*, 15602–15611.

23. Korzhnev, D. M., Salvatella, X., Vendruscolo, M., Di Nardo, A. A., Davidson, A. R., Dobson, C. M., and Kay, L. E. (2004) Low-populated folding intermediates of Fyn SH3 characterized by relaxation dispersion NMR. *Nature 430*, 586–590.

24. Palmer, A. G. (2004) NMR characterization of the dynamics of biomacromolecules. *Chem. Rev. 104*, 3623–3640.

25. Religa, T. L., Markson, J. S., Mayor, U., Freund, S. M., and Fersht, A. R. (2005) Solution structure of a protein denatured state and folding intermediate. *Nature 437*, 1053–1056.

26. Nishimura, C., Dyson, H. J., and Wright, P. E. (2006) Identification of native and non-native structure in kinetic folding intermediates of apomyoglobin. *J. Mol. Biol. 355*, 139–156.

27. Feng, H., Zhou, Z., and Bai, Y. (2005) A protein folding pathway with multiple folding intermediates at atomic resolution. *Proc. Natl. Acad. Sci. U.S.A. 102*, 5026–5031.

28. van Mierlo, C. P., van den Oever, J. M., and Steensma, E. (2000) Apoflavodoxin (un)folding followed at the residue level by NMR. *Protein Sci. 9*, 145–157.

29. Schulman, B. A., Kim, P. S., Dobson, C. M., and Redfield, C. (1997) A residue-specific NMR view of the non-cooperative unfolding of a molten globule. *Nat. Struct. Biol. 4*, 630–634.

30. Cavanagh, J. (1996) Protein NMR spectroscopy: Principles and practice, Academic Press, San Diego.

31. Warren, J. R., and Gordon, J. A. (1966) On the Refractive Indices of Aqueous Solutions of Urea. *J. Phys. Chem. 70*, 297–300.

32. Wang, A., and Bolen, D. W. (1997) A naturally occurring protective system in urea-rich cells: Mechanism of osmolyte protection of proteins against urea denaturation. *Biochemistry 36*, 9101–9108.

33. Niranjanakumari, S., Kurz, J., and Fierke, C. (1998) Expression, purification and characterization of the recombinant ribonuclease P protein component from *Bacillus subtilis*. *Nucleic Acids Res. 26*, 3090–3096.

34. Edelhoch, H. (1967) Spectroscopic determination of tryptophan and tyrosine in proteins. *Biochemistry 6*, 1948–1954.

35. Löhr, F., and Rüterjans, H. (1995) A new triple-resonance experiment for the sequential assignment of backbone resonances in proteins. *J. Biomol. NMR 6*, 189–197.

36. Ikura, M., Kay, L. E., and Bax, A. (1990) A novel approach for sequential assignment of ^{1}H, ^{13}C, and ^{15}N spectra of proteins: Heteronuclear triple-resonance three-dimensional NMR spectroscopy. Application to calmodulin. *Biochemistry 29*, 4659–4667.

37. Yamazaki, T., Lee, W., Arrowsmith, C. H., Muhandiram, D. R., and Kay, L. E. (1994) A Suite of Triple Resonance NMR Experiments for the Backbone Assignment of ^{15}N, ^{13}C, ^{2}H Labeled Proteins with High Sensitivity. *J. Am. Chem. Soc. 116*, 11655–11666.

38. Grzesiek, S., and Bax, A. (1992) Correlating backbone amide and side chain resonances in larger proteins by multiple relayed triple resonance NMR. *J. Am. Chem. Soc. 114*, 6291–6293.

39. Grzesiek, S., Anglister, J., and Bax, A. (1993) Correlation of Backbone Amide and Aliphatic Side-Chain Resonances in ^{13}C/^{15}N-Enriched Proteins by Isotropic Mixing of ^{13}C Magnetization. *J. Magn. Reson., Ser. B 101*, 114–119.

40. Lyons, B. A., and Montelione, G. T. (1993) An HCCNH Triple-Resonance Experiment Using Carbon-13 Isotropic Mixing for Correlating Backbone Amide and Side-Chain Aliphatic Resonances in Isotopically Enriched Proteins. *J. Magn. Reson., Ser. B 101*, 206–209.

41. Delaglio, F., Grzesiek, S., Vuister, G. W., Zhu, G., Pfeifer, J., and Bax, A. (1995) NMRPipe: A multidimensional spectral processing system based on UNIX pipes. *J. Biomol. NMR 6*, 277–293.

42. Johnson, B. A., and Blevins, R. A. (1994) NMR View: A computer program for the visualization and analysis of NMR data. *J. Biomol. NMR 4*, 603–614.

43. Henkels, C. H., Kurz, J. C., Fierke, C. A., and Oas, T. G. (2001) Linked folding and anion binding of the *Bacillus subtilis* ribonuclease P protein. *Biochemistry 40*, 2777–2789.

44. Berg, J. M., Tymoczko, J. L., and Stryer, L. (2002) Biochemistry, 5th ed., W. H. Freeman, New York.

45. Kim, S., Bracken, C., and Baum, J. (1999) Characterization of millisecond time-scale dynamics in the molten globule state of α-lactalbumin by NMR. *J. Mol. Biol. 294*, 551–560.

46. McConnell, H. M. (1958) Reaction Rates by Nuclear Magnetic Resonance. *J. Chem. Phys. 28*, 430–431.

47. Wittekind, M., and Mueller, L. (1993) HNCACB, a High-Sensitivity 3D NMR Experiment to Correlate Amide-Proton and Nitrogen Resonances with the α- and β-Carbon Resonances in Proteins. *J. Magn. Reson., Ser. B 101*, 201–205.

48. Wishart, D. S., and Sykes, B. D. (1994) The ^{13}C chemical-shift index: A simple method for the identification of protein secondary structure using ^{13}C chemical-shift data. *J. Biomol. NMR 4*, 171–180.

49. Spera, S., and Bax, A. (1991) Empirical correlation between protein backbone conformation and Cα and Cβ ^{13}C nuclear magnetic resonance chemical shifts. *J. Am. Chem. Soc. 113*, 5490–5492.

50. Shen, Y., Delaglio, F., Cornilescu, G., and Bax, A. (2009) TALOS+: A hybrid method for predicting protein backbone torsion angles from NMR chemical shifts. *J. Biomol. NMR 44*, 213–223.

51. Stams, T., Niranjanakumari, S., Fierke, C., and Christianson, D. (1998) Ribonuclease P protein structure: Evolutionary origins in the translational apparatus. *Science 280*, 752–755.

52. Solomon, I. (1955) Relaxation Processes in a System of Two Spins. *Phys. Rev. 99*, 559.

53. Bloembergen, N., and Morgan, L. O. (1961) Proton Relaxation Times in Paramagnetic Solutions. Effects of Electron Spin Relaxation. *J. Chem. Phys. 34*, 842–850.

54. Inagaki, F., Watanabe, K., and Miyazawa, T. (1979) Hexacyanochromate ion as a paramagnetic anion probe for active sites of enzymes. Application to ribonuclease A. *J. Biochem. 86*, 591–594.

55. Fairbrother, W. J., Graham, H. C., and Williams, R. J. (1990) An NMR study of anion binding to yeast phosphoglycerate kinase. *Eur. J. Biochem. 190*, 161–169.

56. Henkels, C. H., and Oas, T. G. (2006) Ligation-state hydrogen exchange: Coupled binding and folding equilibria in ribonuclease P protein. *J. Am. Chem. Soc. 128*, 7772–7781.

57. Niranjanakumari, S., Day-Storms, J. J., Ahmed, M., Hsieh, J., Zahler, N. H., Venters, R. A., and Fierke, C. A. (2007) Probing the architecture of the *B. subtilis* RNase P holoenzyme active site by cross-linking and affinity cleavage. *RNA 13*, 521–535.

58. Crary, S., Niranjanakumari, S., and Fierke, C. (1998) The protein component of *Bacillus subtilis* ribonuclease P increases catalytic efficiency by enhancing interactions with the 5′ leader sequence of pre-tRNAAsp. *Biochemistry 37*, 9409–9416.

59. Niranjanakumari, S., Stams, T., Crary, S., Christianson, D., and Fierke, C. (1998) Protein component of the ribozyme ribonuclease P alters substrate recognition by directly contacting precursor tRNA. *Proc. Natl. Acad. Sci. U.S.A. 95*, 15212–15217.